MONTE CARLO SIMULATION OF MEASUREMENT UNCERTAINTY IN MODIFIED HYDRAULIC BULGING DETERMINATION OF FLOW STRESS

Petar Piljek, Biserka Runje, Zdenka Keran, Marko Škunca

Original scientific paper

In this paper an estimation of measurement uncertainty in determining the flow stress curve by modified hydraulic bulging was carried out. Modified hydraulic bulging is a newer method of the stress-strain diagram acquisition. The method has been derived from the hydraulic bulge test. The flow stress-strain curves were established for an aluminium sheet on an experimental apparatus designed for both methods. The assumption of the membrane stress state was used and the flow rule was determined, which was necessary for establishing the flow stress-true strain curve. The comparison between the experimentally obtained curve and standard true stress – true strain curve from literature is showed on a diagram. The estimation of measurement uncertainty was performed using the Monte Carlo simulation.

Keywords: flow stress curve; measurement uncertainty; modified hydraulic bulging; Monte Carlo simulation

Monte Carlo simulacija u procjeni mjerne nesigurnosti krivulje plastičnog tečenja dobivene modificiranim hidrauličkim udubljivanjem

Izvorni znanstveni članak

U radu je provedena procjena mjerne nesigurnosti rezultata mjerenja korištenih za određivanja krivulje plastičnog tečenja u postupku modificiranog hidrauličnog udubljivanja. Postupak modificiranog hidrauličnog udubljivanja je novo razvijena metoda koja služi za snimanje krivulje plastičnog tečenja materijala, a temelji se na klasičnom postupku hidrauličnog udubljivanja. Na eksperimentalnom postavu pomoću kojeg je moguće provesti oba navedena postupka snimljena je krivulja plastičnog tečenja aluminija. Pretpostavljeno je membransko stanje naprezanja materijala te je izveden uvjet plastičnog tečenja materijala koji je neophodan za snimanje krivulje plastičnog tečenja. Eksperimentalno dobivena krivulja plastičnog tečenja uspoređena je sa standardiziranom krivuljom plastičnog tečenja. Procjena mjerne nesigurnosti provedena je primjenom Monte Carlo simulacije.

Ključne riječi: krivulja plastičnog tečenja; mjerna nesigurnost; modificirano hidraulično udubljivanje; Monte Carlo simulacija

1 Introduction

By the definition flow stress curve yields unique and nonlinear relation between true stress and true strain in material. Since both strain and stress are tensors, their degradation to scalars, besides the analytical exactness of this transformation [1], introduces an error to the flow stress curve. The result of this is a great dissipation of curves for the same material when curve acquisition is performed through different methods. Therefore authors [2, 3, 4] inaugurate the use of hydraulic bulging in recording of the true stress – true strain curve.

From the experimental work of [5] and analytical work of [2] hydraulic bulging was constantly developing [6, 7], but has never attained the popularity of standard acquisition methods of true stress – strain curves [3]. Reason to this is dependency of the true stress upon geometrical assumptions set on bulge geometry. Some authors have conducted detailed research on geometry of the bulge and thickness distribution [3, 7] putting the emphasis on strain determination.

Kinematics of *modified* hydraulic bulging imposes on the implementation of a hypothesis stating that equivalent strain in every point of the body can be defined by measuring only the change in sheet thickness [8, 9]. According to that, Hill's hypothesis [10] of equality of circular and meridional deformation in points O and K will be accepted, while in the point of maximal thinning E it will be supposed that circular deformation i.e. strain is equal to zero ($\varphi_c = 0$). Of course, in every point of the deforming sheet the incompressibility assumption is valid. The only, but essential, difference between the classical and the modified hydraulic bulging is in the sphere positioned above the deforming blank, as shown in Fig. 1.

Deforming pressure p "pushes" the sheet onto the sphere with a force F that is produced by a force transducer positioned in the axis of symmetry above the sphere.
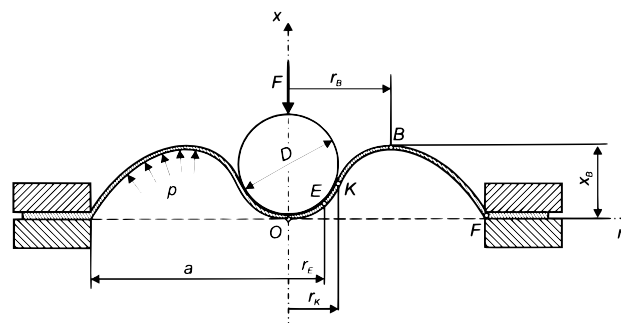

Figure 1 Schematic diagram of modified hydraulic bulging [8]

In the procedure of measuring the equivalent stress and thickness strain there are numerous factors that significantly influence the uncertainty of measurement. The main sources of uncertainty that contribute to the uncertainty of measurement results are listed as follows:

- measuring instrument used in the measurement procedure,
- the standard for instrument fine tuning,
- the repeatability and reproducibility of the instrument positioning,
- the geometry of the surface of the measured object (curvature of the surface, out of flatness, surface roughness etc.),
- temperature influence.

Generally, the uncertainty is calculated for a very specific measurement procedure. The specificity of the measuring procedure and the factors of influence must be

unambiguously defined before the determination of uncertainty.

2 Stress in modified bulging
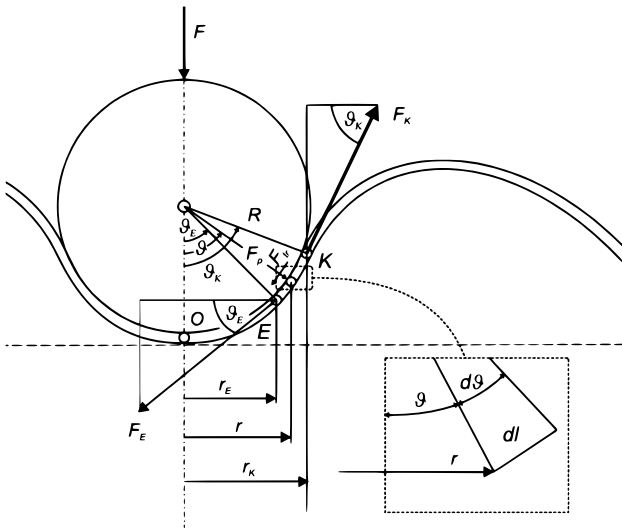### 2.1 Stress at point K

Figure 2 Detailed diagram of forces and geometry in the calculation of stress at point *E* [8]

From the geometry of the deformed blank, diameter D_K, angle ϑ_K, shown in Fig. 2, and the sheet thickness at point K, true meridional stress $\sigma_{m,K}$ can be calculated at point K as

$$\sigma_{m,K} = \frac{F_K}{A_K} = \frac{F}{A_K \sin \vartheta_K} = \frac{2R \cdot F}{\pi \cdot s_K \cdot D_K^2 \cdot \left(1 + \frac{s_K}{2R}\right)}, \text{MPa} \quad (1)$$

Here, F_K = force in direction of the normal at point K, A_K = area of normal cross-section of the sheet at point K, F = the force produced by the transducer, ϑ_K = angle between the axis of symmetry and the normal at point K, R = radius of the sphere, s_K = sheet thickness at point K and D_K = diameter at point K (Fig. 2). Since point K lies on the sphere, the radial and the meridional curvature are the same, and consequently circular stress $\sigma_{c,K}$ can be calculated from well-known membrane or Laplace equation as

$$\sigma_{c,K} = \frac{p_K}{s_K} R - \sigma_{m,K}, \text{MPa} \quad (2)$$

where s_K = thickness at point K, R = radius of the sphere and p_K = pressure at point K calculated as

$$p_K = p_{CNT} - p = \frac{4F}{D_K^2 \pi} - p, \text{MPa} \quad (3)$$

Here p_{CNT} = contact pressure between sheet and the sphere at point K and p = deforming pressure.

The required true stress is equal to equivalent von Mises stress. At point K, equivalent von Mises stress, $\sigma_{ekv,K}$, is calculated from the meridional, circular and the normal stress as follows

$$\sigma_{ekv,K} = \left\{ \frac{1}{2} \left[(\sigma_{m,K} - \sigma_{c,K})^2 + (\sigma_{m,K} - \sigma_{n,K})^2 + (\sigma_{c,K} - \sigma_{n,K})^2 \right] \right\}, \text{MPa} \quad (4)$$

where $\sigma_{n,K}$ = normal stress at point K, which is calculated as a mean value of contact pressure p_{CNT} and deforming pressure p:

$$\sigma_{n,K} = -\frac{1}{2}(p_{CNT} + p). \text{MPa} \quad (5)$$

2.2 Stress at point E

Point E is the point of maximal thinning of the sheet in modified bulging. Therefore, the equilibrium of forces in radial direction r between points K and E gives

$$\sum F_r = 0, \text{N} \quad (6)$$

$$-F_E \cos(\vartheta_E) - F_{tr}\cos(\vartheta) + F_p \sin(\vartheta) + F_K \cos(\vartheta_K) = 0 \quad (7)$$

resulting in the force at point E calculated as:

$$F_E = \frac{1}{\cos\vartheta_E} \left\{ F_K \cos\vartheta_K - p_K R^2 \pi \mu [\cos(2\vartheta_K) - \cos(2\vartheta_E)] + 2p_K R^2 \pi \left\{ \left[\vartheta_K - \frac{1}{2}\sin(2\vartheta_K) \right] - \left[\vartheta_E - \frac{1}{2}\sin(2\vartheta_E) \right] \right\} \right\}, \text{N} \quad (8)$$

Friction factor was taken to be $\mu = 0{,}2$. The meridional force divided by the area of normal cross – section of sheet A_E at point E is equal to stress:

$$\sigma_{m,E} = \frac{F_E}{A_E} = \frac{F_E}{\pi \cdot s_E \cdot D_E \left(1 + \frac{s_E}{2R}\right)}, \text{MPa} \quad (9)$$

Point E lies on the sphere, and consequently the radial and the meridional curvature are the same and the circular stress is calculated from membrane equation as:

$$\sigma_{c,E} = \frac{p_K}{s_E} R - \sigma_{m,E}, \text{MPa} \quad (10)$$

where p_K is pressure in point E which is the same as pressure in point K.

Normal stress at point E is the same as normal stress at point K (see above). According to that, the equivalent stress at point E is given as:

$$\sigma_{ekv,E} = \left\{ \frac{1}{2} \left[(\sigma_{m,E} - \sigma_{c,E})^2 + (\sigma_{m,E} - \sigma_{n,E})^2 + (\sigma_{c,E} - \sigma_{n,E})^2 \right] \right\}^{\frac{1}{2}}, \text{MPa} \quad (11)$$

2.3 Stress at point O

Using the assumption of equal meridional and circular stress at the pole $\sigma_m = \sigma_c$ (commonly used for the

stress at the pole in hydraulic bulging [2, 5, 6, 7]), known thickness s_O and meridional and circular radius equal to the radius of the sphere R, and substituting these into membrane equation it is possible to find the plane stress at point O as:

$$\sigma_{m,c,O} = \frac{p_K}{2\,s_O}R\ ,\ \text{MPa} \tag{12}$$

where p_K is the same pressure as given for point K. Normal stress at point O equals normal stress at point K as it has been previously calculated. Therefore, the equivalent stress at point O equals:

$$\sigma_{ekv,O} = \left|\sigma_{m,c,O} - \sigma_{n,O}\right|,\ \text{MPa} \tag{13}$$

3   Strain in modified bulging

In order to record the true stress – strain diagram, the equivalent strain has to be determined for points K, E, and O. In order to simplify the measurements, equivalent strain is determined from thickness strain, i.e. from the normal cross-section at each of the points. Using the strain ratio $\beta = \varphi_2/\varphi_1$ ($\varphi_1 > \varphi_2$) [5], the relation between the equivalent and the thickness strain is given as:

$$\varphi_{ekv} = \frac{2}{1+\beta}\sqrt{\frac{1+\beta+\beta^2}{3}}\varphi_3\ , \tag{14}$$

Where $\varphi_3 = \ln(s_0/s_1)$ is the thickness strain for points K, E, or O. s_0 is the initial and s_1 is the final sheet thickness. The strain ratio β in Eq. (14) stands for the logarithmic strains $\beta = \varphi_2/\varphi_1$, as previously mentioned. For points K and O it is assumed that the straining process is proportional, i.e. $\beta = 1$. Hence, the equivalent strain at points K and O is equal to the thickness strain, which simplifies the measurements.

$$\varphi_{ekv,K,O} = \varphi_3 \tag{15}$$

The same assumption was made for classical hydraulic bulging where strain is measured at the pole.

For point E as the point of maximal thinning, the assumption of the plane strain was made by giving $\beta = 0$. Inserting $\beta = 0$ in Eq. (14) results in

$$\varphi_{ekv,E} = \frac{2}{\sqrt{3}}\varphi_3 \tag{16}$$

In modified hydraulic bulging with no draw in allowed, the strain ratio β can only reach values between 0 (plane strain) and 1 (equal biaxial stretching). Since the values of the function given by Eq. (14) are monotonically decreasing from the value $2/\sqrt{3}\varphi_3$ at $\beta = 0$ to the value φ_3 at $\beta = 1$, the equivalent strain is always within the interval

$$\varphi_{ekv} \in \left[1....\frac{2}{\sqrt{3}}\right]\varphi_3 \tag{17}$$

In the presented case of modified hydraulic bulging on the sphere, two cases of strain were considered:
1. For points K and O, equal biaxial stretching $\beta = 1$ was assumed.
2. For point E, plane strain $\beta = 0$ was assumed.

These assumptions resulted in the true stress-strain curve recorded for a 1 mm thick Al 99,5 sheet [8], shown in Fig. 3.

4   Calculating measurement uncertainty

A measurement result is generally expressed as a single measurand quantity value and a measurement uncertainty. According to the International vocabulary of metrology, measurement uncertainty is defined as a parameter that describes the dispersion of quantity values that could reasonably be attributed to the measurand. The uncertainty of the measurement result reflects the lack of complete knowledge about the value of the measurand. In this paper the measurement uncertainty evaluation has been carried out using the Monte Carlo simulations (MCS method) in accordance with the document JCGM 101:2008. The Monte Carlo simulation (MCS method) is a statistic simulation based on use of random numbers and probability statistics [9÷19]. In the procedure of the measurement uncertainty estimation, MSC method generates random numbers from the probability density function for every input quantity x_i and forms the corresponding value of the output quantity y, combining various distributions by which input quantities are defined. The procedure is repeated M times and thus an experimental probability density function of the output quantity is reached. For the level of confidence P, estimation of the output quantity y, estimated standard deviation, and the coverage interval $(y_{\left(\left(\frac{1-P}{2}\right)\cdot M\right)}, y_{\left(\left(\frac{1+P}{2}\right)\cdot M\right)})$ are obtained from the experimental probability density function.
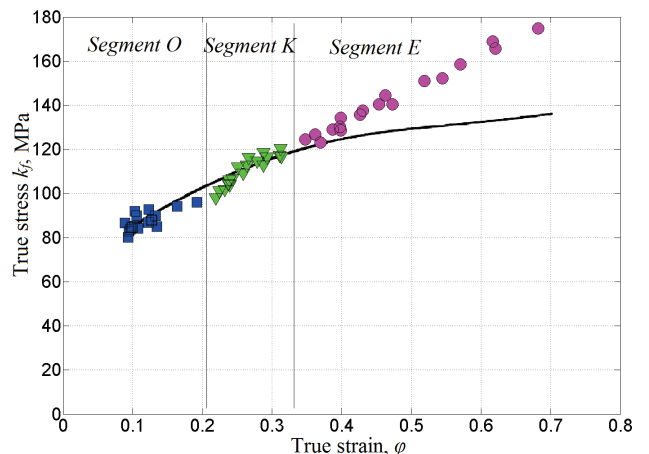

Figure 3 True stress – true strain curve obtained in modified hydraulic bulging experiment compared to true stress – true strain curve from literature [3]

The probability density functions of equivalent stress and of thickness strain for the K, E and O points, are simulated by the MCS method which is based on Eqs. (1) ÷ (16). The probability density functions are obtained by the convolution of the input values distribution with M = 100 000 simulations.

The input values x_i are defined with the probability density functions $g(x_i)$ as shown in Tab. 1 and Tab. 2. The probability density functions of the output values $\sigma_{ekv,K}$, $\sigma_{ekv,E}$ and $\sigma_{ekv,O}$ are presented in Fig. 4(a, b, c). The estimated standard deviations, intervals and expanded uncertainties of the $\sigma_{ekv,K}$, $\sigma_{ekv,E}$ and $\sigma_{ekv,O}$ values are presented in Tab. 3.The probability density functions of the output values $\varphi_{ekv,K}$, $\varphi_{ekv,E}$ and $\varphi_{ekv,O}$ are presented in Fig. 5(a, b, c). The estimated standard deviations, coverage intervals and expanded uncertainties of the output values $\varphi_{ekv,K}$, $\varphi_{ekv,E}$ and $\varphi_{ekv,O}$ are presented in Tab. 4.

Table 1 Input values and probability density functions in simulating of values $\sigma_{ekv,K}$, $\sigma_{ekv,E}$ and $\sigma_{ekv,O}$

Input value x_i		Probability density function $g(x_i)$
Deforming pressure at points K, E, O	p	Rectangular distribution ($18,838 \times 10^5$ Pa; $19,162 \times 10^5$ Pa)
Force at transducer	F	Normal distribution (6 kN; 15 N)
Radius of the sphere	R	Normal distribution (15 mm; 20 μm)
Diameter at point K	D_K	Normal distribution (29,27 mm; 20 μm)
Diameter at point K	D_E	Normal distribution (29,71 mm; 20 μm)
Friction coefficient	μ	Rectangular distribution (-0,1; 0,1)
Sheet thickness at point K	s_K	Normal distribution (0,789 mm; 2,5 μm)
Sheet thickness at point E	s_E	Normal distribution (0,731 mm; 2,5 μm)
Sheet thickness at point O	s_O	Normal distribution (0,905 mm; 2,5 μm)

Table 2 Input values and probability density functions in simulating of values $\varphi_{ekv,K}$, $\varphi_{ekv,E}$ and $\varphi_{ekv,O}$

Input value x_i		Probability density function $g(x_i)$
Initial sheet thickness	s_0	Normal distribution (1,000 mm; 2,5 μm)
Sheet thickness at point K	s_K	Normal distribution (0,789 mm; 2,5 μm)
Sheet thickness at point E	s_E	Normal distribution (0,731 mm; 2,5 μm)
Sheet thickness at point O	s_O	Normal distribution (0,905 mm; 2,5 μm)

a) ($\sigma_{ekv,K}$), MPa   b) $g(\sigma_{ekv,E})$, MPa   c) $g(\sigma_{ekv,O})$, MPa
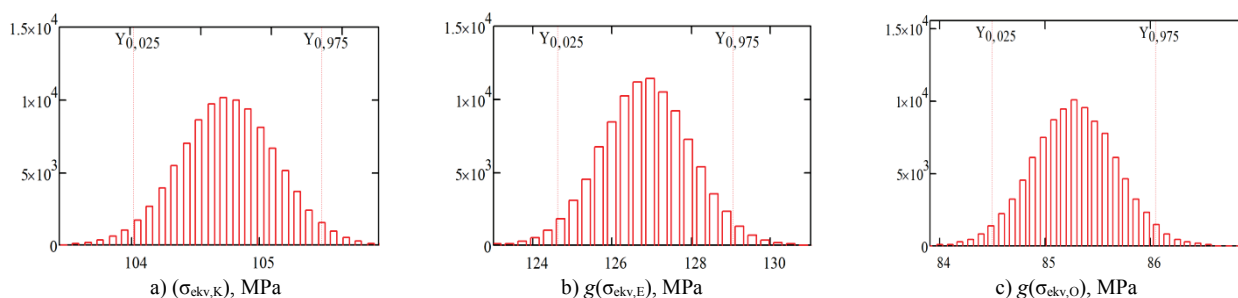
Figure 4 Probability density functions $g(\sigma_{ekv,K})$, $g(\sigma_{ekv,E})$ and $g(\sigma_{ekv,O})$

Table 3 The estimated standard deviations, coverage intervals and expanded uncertainties of the output values $\sigma_{ekv,K}$, $\sigma_{ekv,E}$ and $\sigma_{ekv,O}$

	$\sigma_{ekv,K}$	$\sigma_{ekv,E}$	$\sigma_{ekv,O}$
The estimated standard deviation	2,0 MPa	1,12 MPa	0,4 MPa
Interval of the output value	($y_{0,025}$ = 104,03 MPa, $y_{0,975}$ = 105,47 MPa) k = 2 P = 95 %	($y_{0,025}$ = 124,65 MPa, $y_{0,975}$ = 129,07 MPa) k = 2 P = 95 %	($y_{0,025}$ = 84,49 MPa, $y_{0,975}$ = 86,05 MPa) k = 2 P = 95 %
Expanded uncertainty	U = 0,7 MPa k =2 P = 95 %	U = 2,21 MPa k =2 P = 95 %	U = 0,8 MPa k =2 P = 95 %

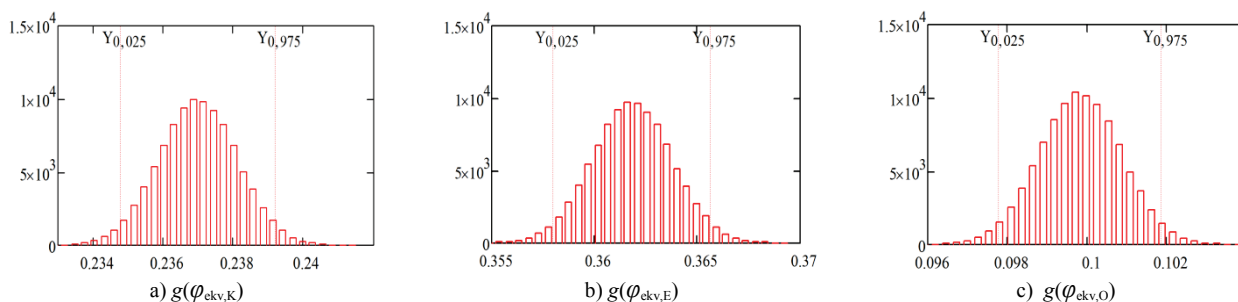a) $g(\varphi_{ekv,K})$ b) $g(\varphi_{ekv,E})$ c) $g(\varphi_{ekv,O})$

Figure 5 Probability density functions $g(\varphi_{ekv,K})$, $g(\varphi_{ekv,E})$, $g(\varphi_{ekv,O})$

Table 4 The estimated standard deviations, intervals and expanded uncertainties of the output values $\varphi_{ekv,K}$, $\varphi_{ekv,E}$ and $\varphi_{ekv,O}$

	$\varphi_{ekv,K}$	$\varphi_{ekv,E}$	$\varphi_{ekv,O}$
The estimated standard deviation	$1{,}13 \times 10^{-3}$	$1{,}95 \times 10^{-3}$	$1{,}04 \times 10^{-3}$
Interval of the output value	$(y_{0,025} = 0{,}235, y_{0,975} = 0{,}239)$ $k = 2$ $P = 95\%$	$(y_{0,025} = 0{,}358, y_{0,975} = 0{,}366)$ $k = 2$ $P = 95\%$	$(y_{0,025} = 0{,}098, y_{0,975} = 0{,}102)$ $k = 2$ $P = 95\%$
Expanded uncertainty	$U = 2{,}2 \times 10^{-3}$ $k = 2;$ $P = 95\%$	$U = 3{,}8 \times 10^{-3}$ $k = 2;$ $P = 95\%$	$U = 2 \times 10^{-3}$ $k = 2;$ $P = 95\%$

5 Conclusion

Modified bulging is a new method of stress-strain curve acquisition. For the purpose of testing of the method, only one material, aluminium Al 99,5 was used. In the analysis of the proposed method the membrane state of stress was presumed. Supposition on strain ratio $\beta = 0$ at point E holds only for the ultimate pressures. Experimental results show the difference of 15 % toward stress-strain curve in literature [3]. Since equivalent strain is additive value regarding strain path, further study of modified hydraulic bulging has to consider strain history at point E.

Interesting detail to be considered is a possibility to perform modified hydraulic bulging without a force transducer, using only assumption of the membrane stress at point B. Since there is no thickness stress, exerted force onto the surface of radius r_B by pressure p, equals the force F on the sphere, shown in Fig. 1. It is supposed that some standardization of the method in future has to be established.

The relative measurement uncertainties regarding stress is maximum for the segment E where it is up to 1,8 % while maximum strain relative measurement uncertainties is obtained for segment O where it is up to 2,25 %. Based on the evaluated measurement uncertainties, it can be concluded that the measurement system is capable of detecting changes in the hydraulic bulging process.

6 References

[1] Kachanov, L. M. Fundamentals of the Theory of Plasticity. Mir Publishers, Moscow, 1974.

[2] Hill, R. A theory of plastic bulging of a metal diaphragm by lateral pressure. // Phil. Mag. 41(1950), pp. 1133-1142. DOI: 10.1080/14786445008561154

[3] Doege, E.; Meyer-Nolkemper, H.; Saeed, I. Fliesskurvenatlas metallischer Werkstoffe. Hanser Verlag, München Wien, 1986.

[4] Brown, W. F.; Thompson, F. C. Strength and failure characteristics of metal membranes in circular bulging. // Transactions of ASME. 71(1949), pp. 557-585.

[5] Gleyzal, A. Plastic deformation of circular diaphragm under pressure // Journal of Applied Mechanics. 70(1948), pp. 288-296.

[6] Bell, R.; Duncan, J. L.; Wilson, I. H. A sheet bulging machine with closed loop control. // Journal of Strain Analysis. 2(1967), pp. 246-253. DOI: 10.1243/03093247V023246

[7] Fliesskurven Atlas // Untersuchungen der hydraulischen Tiefung zur Aufnahme von Fliesskurven an Blechwerkstoffen. // Industrie Anzeiger. 90, 38(1968), pp. 775-779.

[8] Škunca, M. Modified hydraulic bulging on the sphere. // PhD work, University of Zagreb, 2009.

[9] Keran, Z.; Math, M.; Škunca, M. Determination of Flow stress Curve by Modified Hydraulic Bulging. // Transactions of FAMENA. 35(2011), pp. 13-26.

[10] Bendato I.; Cassettari L.; Mosca M.; Mosca R.; Rolando F. New Markets Forecast and Dynamic Production Redesign Through Stochastic Simulation. // International Journal of Simulation Modelling. 14, 3(2015), pp. 485-498. DOI: 10.2507/IJSIMM14(3)10.307

[11] Gusell, A.; Acko, B.; Mudronja, V. Measurement Uncertainty in Calibration of Measurement Surface Plates Flatness. // Strojniski vestnik-Journal of Mechanical Engineering. 55, 5(2009), pp. 286-292.

[12] Madić M.; Radovanović M.; Manić M.; Trajanović M. Optimization of CO_2 Laser Cutting Process using Taguchi and Dual Response Surface Methodology. // Tribology in Industry. 36, 3(2014), pp. 236-243.

[13] Primorac, B. B.; Parunov, J. Probabilistic models of reduction in ultimate strength of a damaged ship. // Transactions of FAMENA. 39, 2(2015), pp. 55-74.

[14] Kleiner, M.; Geiger, M.; Klaus, A. Manufacturing of lightweight components by metal forming. // CIRP Annals - Manufacturing Technology. 52(2003), pp. 521-542. DOI: 10.1016/S0007-8506(07)60202-9

[15] Ranta-Eskola, A. J. Use of the hydraulic bulge test in biaxial tensile testing. // International Journal Mechanical Sciences. 21(1979), pp. 457-465. DOI: 10.1016/0020-7403(79)90008-0

[16] JCGM 200:2008 International vocabulary of metrology — Basic and general concepts and associated terms (VIM).

[17] JCGM 100:2008 Evaluation of measurement data — Guide to the expression of uncertainty in measurement.

[18] JCGM 101:2008 Evaluation of measurement data — Supplement 1 to the "Guide to the expression of uncertainty in measurement" — Propagation of distributions using a Monte Carlo method.

[19] Medić, S.; Kondić, Ž.; Runje, B. Validation of the Realised Measurement Uncertainty in Process of Precise Line Scales Calibration. // Technical Gazette. 19, 2(2012), pp. 331-337.

Authors' addresses

Petar Piljek, Ph.D. Student
Department of Technology, Faculty of Mechanical Engineering and Naval Architecture, University of Zagreb, Croatia
Ivana Lučića 5, 10002 Zagreb, Croatia
E-mail: petar.piljek@fsb.hr

Prof. Biserka Runje, Ph.D.
Department of Quality, Faculty of Mechanical Engineering and Naval Architecture, University of Zagreb, Croatia
Ivana Lučića 5, 10002 Zagreb, Croatia
E-mail: biserka.runje@fsb.hr

Zdenka Keran, Ph.D.
Department of Technology, Faculty of Mechanical Engineering and Naval Architecture, University of Zagreb, Croatia
Ivana Lučića 5, 10002 Zagreb, Croatia
E-mail: zdenka.keran@fsb.hr

Marko Škunca, Ph.D.
Alstom, Dubrovačka 45, 10312 Predavec
E-mail: skunca.marko@gmail.com

BEM/MRM 40

40th International Conference on Boundary Elements and other Mesh Reduction Methods
12 – 14 September 2017
New Forest, UK

Organised by
Wessex Institute, UK
University of Mississippi, USA

Sponsored by
WIT Transactions on Engineering Sciences
International Journal of Computational Methods and Experimental Measurements

witconferences.com/bem40

CALL FOR PAPERS

WIT CONFERENCES

Location

BEM/MRM 40 will be held in the New Forest National Park, which borders the south coast of England and is home to the Wessex Institute. The New Forest is situated in central southern England, 100km from London. Spreading over nearly 400 square kilometres, this National Park is home to picturesque villages, unspoiled scenery, abundant wildlife and many attractions for visitors.

The New Forest was established as a royal hunting ground by the Norman King William I, and 900 years later, the New Forest is still owned by the Crown. Local commoners have the right to graze their ponies, cattle and pigs on forest land where they wander freely. The Forest is unarguably recognised as one of the most unique wilderness areas in Western Europe, where many landscapes have remained virtually unchanged for many centuries.

Conference Venue

Situated at the heart of the New Forest National Park, the Balmer Lawn Hotel has uniquely designed and decorated rooms. This 4 star hotel has its own restaurant, 3 acres of grounds, squash courts, tennis court, pools, sauna, spa and fitness suite as well as direct access to the New Forest. Only a short walk from the shops, pubs and restaurants of Brockenhurst village and Brockenhurst train station, the hotel is easily accessible.

Submission Information

Abstracts of no more than 300 words should be submitted as soon as possible.

Abstracts should clearly state the purpose, results and conclusions of the work to be described in the final paper. Final acceptance will be based on the full-length paper, which if accepted for publication must be presented at the conference.

The language of the conference will be English.

Online submission:
www.witconferences.com/bem2017

Conference Secretariat
Irene Moreno Millan
imoreno@wessex.ac.uk

Wessex Institute
Ashurst Lodge, Ashurst
Southampton, SO40 7AA, UK

Tel: +44 (0) 238 029 3223
Fax: +44 (0) 238 029 2853

For more information visit: **www.witconferences.com/bem40**

Front Image © Michael Keen Flickr

The annual conference on Boundary Elements and other Mesh Reduction Methods (BEM/MRM) started in 1978 and is now in its 40th version. It is well established as the recognised international forum for the latest advances in those techniques and their application in science and engineering.

The objective of the research papers presented at the meetings is the further development of techniques that reduce or eliminate the type of meshes required by first generation computational methods, such as finite differences or finite elements.

This has steadily been achieved through the development of BEM as a computational tool and continues through more recent research into advanced techniques. The meeting also encourages the presentation of papers on the use of BEM and, in particular, the description of new applications. Problems related to interface with other techniques, processes such as finite elements, the solution of large systems of equations and the direct coupling of BEM to design and manufacturing are also welcome.

All the meetings since 1978 have produced a series of edited volumes in which the major developments in the field have been presented. This valuable collection has been in digital form since 1993 with the papers available Open Access in the Wessex Institute's eLibrary website (http://www.witpress.com/elibrary) where they can be easily accessed and downloaded.

Benefits of Attending

Publication of Papers: Papers are to be published by WIT press in a Volume of WIT Transactions. Selected papers will appear in the International Journal of Computational Methods and Experimental Measurements (ISSN: 2046-0546 Digital ISSN: 2046-0554). Abstracts and papers will be reviewed by members of the Committee and other experts.

Open Access: WIT Press is an advocate of Open Access which offers maximum dissemination of your work. WIT Transactions and Journal papers can be downloaded for free (www.witpress.com/elibrary).

Indexing and Archiving: Papers presented at Wessex Institute conferences are referenced by CrossRef and have appeared in notable reviews and databases. Papers are submitted to various indexing services such as Thomson Reuters Web of Science, Google Scholar, Scopus and ProQuest. All conference books are listed in the British Library and American Library of Congress.

Digital Archive: All conference papers are archived online in the WIT eLibrary (www.witpress.com/elibrary) where they are permanently available to the international community.

Conference Topics

The following list covers some of the topics to be presented at BEM/MRM 40. Papers on other subjects related to the objectives of the conference are also welcome.

Advanced formulations
Advanced meshless and mesh reduction methods
Structural mechanics applications
Solid mechanics
Heat and mass transfer
Electrical engineering and electromagnetics
Computational methods
Fluid flow modelling
Damage mechanics and fracture
Dynamics and vibrations
Engineering applications
Interfacing with other methods
Coupling with design and manufacturing
Solution of large systems of equations

Image: © davidgsteadman Flickr

Conference Chairmen

C A Brebbia
Wessex Institute, UK
A H D Cheng
University of Mississippi, USA

International Scientific Advisory Committee

D E Beskos
University of Patras, Greece
H B Chen
University of Science and Technology of China, China
J T Chen
Taiwan Ocean University, Taiwan
W Chen
Hohai University, China
P Dineva
Bulgarian Academy of Sciences, Bulgaria
E Divo
Embry-Riddle Aeronautical University, USA
N Dumont
PUC-Rio, Brazil
A Galybin
The Schmidt Institute of Physics of the Earth, Russia
X W Gao
Dalian University of Technology, China
L Godinho
University of Coimbra, Portugal
B Y C Hon
City University of Hong Kong, Hong Kong
E Kansa
Convergent Solutions, USA
A Karageorghis
University of Cyprus, Cyprus
A Kassab
University of Central Florida, USA
J Katsikadelis
National Technical University of Athens, Greece
V Leitão
University of Lisbon, Portugal
E Leonel
University of São Paulo, Brazil
D Lesnic
University of Leeds, UK
L Ling
Hong Kong Baptist University, Hong Kong
G Manolis
Aristotle University of Thessaloniki, Greece

L Marin
University of Bucharest, Romania
T Matsumoto
Nagoya University, Japan
A Nowak
Silesian University of Technology, Poland
J B Paiva
University of São Paulo, Brazil
L Palermo Jr
University of Campinas, Brazil
E Pan
University of Akron, USA
D Poljak
University of Split, Croatia
J Ravnik
University of Maribor, Slovenia
J Rencis
Tennessee Tech University, USA
T Rudolphi
Iowa State University, USA
M Schanz
Graz University of Technology, Austria
L Skerget
University of Maribor, Slovenia
V Sladek
Slovak Academy of Sciences, Slovakia
E Strelnikova
National Academy of Sciences of Ukraine, Ukraine
S Syngellakis
Wessex Institute, UK
A Tadeu
UC-ITeCons, Portugal
T Tran-Cong
University of Southern Queensland, Australia
J Trevelyan
University of Durham, UK
V Popov
Ascend Technologies Ltd, UK
O von Estorff
Hamburg-Harburg University of Technology, Germany
P H Wen
Queen Mary University of London, UK
L Wrobel
Brunel University, UK
T Wu
University of Kentucky, USA
J Zhang
Hunan University, China
M Zhao
Zhengzhou University, China

Image © davidgsteadman Flickr